

# Design of a system converting an output radiation of frequency tunable gyrotron into a gaussian beam

メタデータ	言語: English 出版者: 公開日: 2008-02-05 キーワード (Ja): キーワード (En): 作成者: OGAWA, I, IDEHARA, T, SABCHEVSKI, S, KASPAREK, W メールアドレス: 所属:
URL	<a href="http://hdl.handle.net/10098/1541">http://hdl.handle.net/10098/1541</a>

# Design of a system converting an output radiation of frequency tunable gyrotron into a gaussian beam

I. OGAWA†¶, T. IDEHARA‡, S. SABCHEVSKI‡ and  
W. KASPAREK§

A novel design of a versatile quasi-optical system for conversion of gyrotron radiation into collimated gaussian beams is presented and discussed. The proposed system consists of a quasi-optical antenna, two ellipsoidal mirrors and a spatial filter which truncates the sidelobe radiation. The system is appropriate as a transmission line for frequency tunable gyrotrons operating at  $TE_{0n}$  and  $TE_{1n}$  modes. As an illustration of our approach, we present results which demonstrate the applicability of the developed system for conversion of the radiation generated by the Gyrotron FU IVA. The examples include conversion of four  $TE_{1n}$  mode outputs ( $TE_{12}$ , 170 GHz;  $TE_{13}$ , 271 GHz;  $TE_{14}$ , 372 GHz;  $TE_{15}$ , 472 GHz) into gaussian-like beams and three  $TE_{0n}$  modes ( $TE_{02}$ , 223 GHz;  $TE_{03}$ , 323 GHz;  $TE_{04}$ , 423 GHz) into bigaussian-like beams.

## 1. Introduction

High frequency gyrotrons are characterized by their capacity to deliver high powers in the submillimetre wavelength range (Zaytsev *et al.* 1974, Flyagin *et al.* 1983, Spira-Hakkarainen *et al.* 1990, Idehara *et al.* 1995) and their frequency step-tunability due to the alternation of the operating mode (Kreischer and Temkin 1987, Brand *et al.* 1990 b, Idehara *et al.* 1998, Nusinovich and Read 1999). For many applications such as plasma scattering measurements (e.g. Woskoboinikow *et al.* 1983, Terumichi *et al.* 1984, Fekete *et al.* 1994, Suvorov *et al.* 1997) where more intense waves are required, the gyrotrons are the most promising candidates as power sources in this region of the electromagnetic spectrum. Very often the gyrotron output needs to be converted into a gaussian-like beam because the gyrotron generates radiation with  $TE_{mn}$  mode structure, which is far from what is usually required from the radiation power source.

In an earlier paper (Ogawa *et al.* 1997) we presented a quasi-optical system designed to convert the gyrotron output ( $TE_{15}$  mode, 354 GHz) into a gaussian-like beam. In this system, a quasi-optical antenna (Vlasov and Orlova 1974) was used to convert the gyrotron output into a linearly polarized beam. Its far-field consists of sidelobes and a main beam which is similar to a gaussian beam. The

---

† Faculty of Engineering, Fukui University, Fukui 910-8507, Japan.

‡ Research Center for Development of Far-Infrared Region, Fukui University, Fukui 910-8507, Japan.

§ Institut für Plasmaforschung, Universität Stuttgart, Pfaffenwaldring 31, D-70569 Stuttgart, Germany.

¶ Corresponding author. e-mail: ogawa@maxwell.apphy.fukui-u.ac.jp

quality of the produced beam was improved only by focusing the main beam using an ellipsoidal mirror. If we apply this system to other  $TE_{1n}$  modes, the positions and sizes of the beam waist would undergo changes. For most purposes however, a gaussian beam with constant waist size and constant waist position is required.

Over the years a number of step tunable gyrotrons (Gyrotron FU Series) covering a wide frequency range have been developed at Fukui University (Idehara *et al.* 1999). For such gyrotrons, systems capable of converting the outputs from a set of operating modes are required. This motivated us to develop a new more versatile transmission line which converts several  $TE_{0n}$  and  $TE_{1n}$  mode outputs generated by the gyrotron FU IVA (Idehara *et al.* 1998) into well-collimated beams. Although the size of the main beam at the far-field region depends on gyrotron output mode, it is possible to treat it as a bigaussian beam with constant waist located at the antenna (Ogawa *et al.* 1999c). Taking advantage of this approach the objective beam is obtained by using a confocal mirror system with a spatial filter. In this system the first mirror converts the beam produced by the quasi-optical antenna into the far-field, while the filter truncates the sidelobes.

The paper is organized as follows. In § 2 we outline briefly the approach used for calculation of the radiation patterns. The gist of the technique for the system design based on the gaussian optics is depicted in § 3. The results from the calculations using the Huygens equation for scalar diffraction are presented in § 4. The paper concludes with a summary of the capabilities of the developed conversion system.

## 2. Calculation of radiation patterns

If the electromagnetic fields produced by a quasi-optical antenna are known, then those at any subsequent point can be obtained by solving the Helmholtz equation together with the corresponding boundary conditions on each mirror. Another equivalent approach is based on the use of the Huygens equation for scalar diffraction (e.g. Kong 1986). As in our earlier works (Ogawa *et al.* 1997) we follow the latter technique.

The quasi-optical antenna (figure 1) consists of a circular waveguide (internal radius  $a_w = 10$  mm) with a step-cut and a parabolic cylinder reflector (focal length  $f_p = 15.5$  mm). This antenna converts the  $TE_{1n}$  output of the Gyrotron FU IVA into a linearly polarized beam. The electric and magnetic fields are parallel to the  $x$ - and  $y$ -directions, respectively.

It is well known that for all modes except  $TE_{11}$ , the radiation spreads in a hollow cone with a semiangle given by

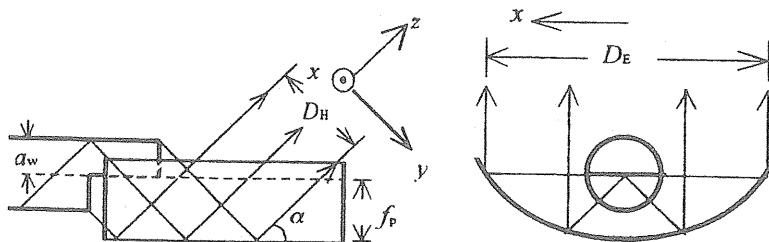


Figure 1. Quasi-optical antenna.

$$\sin \alpha = \frac{k_c}{k} \quad (1)$$

where  $k_c = \rho'_{mn}/a_w$  is the cutoff wavenumber,  $\rho'_{mn}$  is the  $n$ th root of  $J'_m(\rho) = 0$ ,  $a_w$  is the waveguide radius and  $k$  is the wavenumber. In the gyrotron cavity the mode is very close to cutoff and

$$k = k_{\text{cav}} = \frac{\rho'_{mn}}{a_c} \quad (2)$$

where  $a_c$  is the cavity radius. If we neglect mode conversion

$$\alpha = \sin^{-1} \frac{a_c}{a_w} \quad (3)$$

This means that to a first approximation the angle  $\alpha$  is independent of the mode. In our case,  $\alpha = 8.63^\circ$ . The fields over this image source are calculated using the well-known approach based on geometrical optics (Wada and Nakajima 1986, Brand *et al.* 1990 a).

The incident electromagnetic fields at the first mirror are calculated using the Huygens equation. The electromagnetic fields reflected from the mirror are given by the boundary conditions (Ogawa *et al.* 1999 b). The electromagnetic fields on the subsequent mirrors are obtained using repeatedly the Huygens equation and the boundary conditions together with the previously calculated results as the source fields.

### 3. Design of the system using gaussian optics

In order to investigate how the beams spread, their intensity profiles have been calculated for a plane situated far from the image source. The image source is located so that the beam with polarization in the  $x$ -direction propagates along the  $z$ -direction (figure 2). The intensity profiles for  $\text{TE}_{0n}$  modes in the far-field region are shown in figure 3 and those for  $\text{TE}_{1n}$  modes are shown in figure 4.

Each far-field consists of a main beam and additional sidelobes. The main beams for  $\text{TE}_{0n}$  modes have elliptical cross-section and their spot sizes are given by assuming a bigaussian beam whose waist (waist size  $w_{x0} = 26.4$  mm in width and  $w_{y0} = 18.0$  mm in length) is located at the centre of the image source (table 1) (Ogawa *et al.* 1999 c). On the other hand, those for  $\text{TE}_{1n}$  modes are circular and

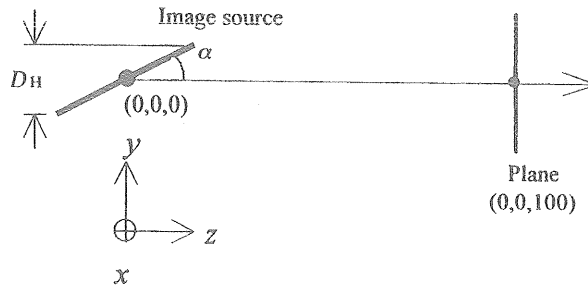


Figure 2. Plane image source used in the calculation of the subsequent radiation patterns of the quasi-optical antenna with a single parabolic reflector. The beam propagates along the  $z$ -axis.

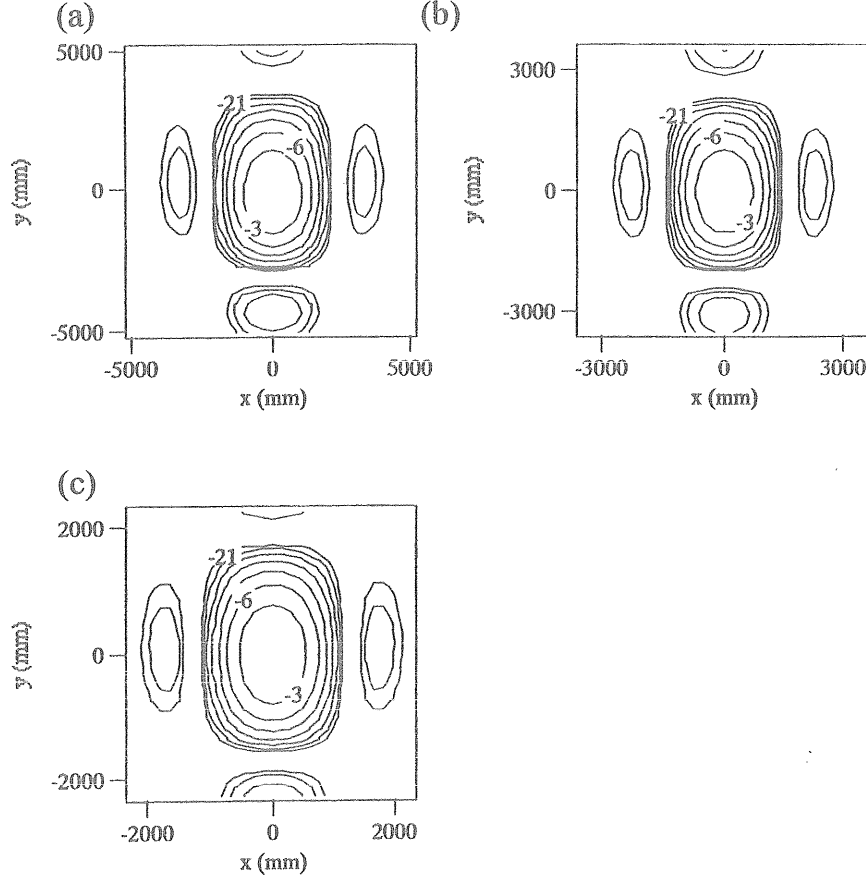


Figure 3. Calculated intensity contours in the far-field region. Distance from the image source is 100 m: (a) TE<sub>02</sub> mode (223 GHz); (b) TE<sub>03</sub> mode (323 GHz); (c) TE<sub>04</sub> mode (423 GHz). Contours are in decibels relative to the intensity maximum.

their spot sizes are given by assuming a gaussian beam with waist size  $w_{x0} = w_{y0} = 18.1$  mm (table 1).

The intensity of the bigaussian beam is given by

$$I = \frac{2P_0}{\pi w_x w_y} \exp\left(-\frac{2x^2}{w_x^2}\right) \exp\left(-\frac{2y^2}{w_y^2}\right) \quad (4)$$

where  $w_x$  and  $w_y$  are the spot sizes in the  $x$ - and  $y$ -directions, respectively and  $P_0$  is the total beam power. We will define the spot size of such a beam as the radius of the  $-8.69$  dB contour, where the intensity is  $e^{-2}$  smaller than at the maximum.

Propagation and focusing of a bigaussian beam is most conveniently treated by the use of the complex beam parameters  $q_x$  and  $q_y$  (e.g. Siegman 1971, Ogawa *et al.* 1999 a).

In the system under consideration (figure 5), the focal length  $f_1$  of the mirror m1 coincides with the distance  $d_1$ , i.e.  $f_1 = d_1 = 1.5$  m. For this special arrangement, the far-field of the image source appears in the  $y = 1.241$  plane (Ogawa *et al.* 1999 b).

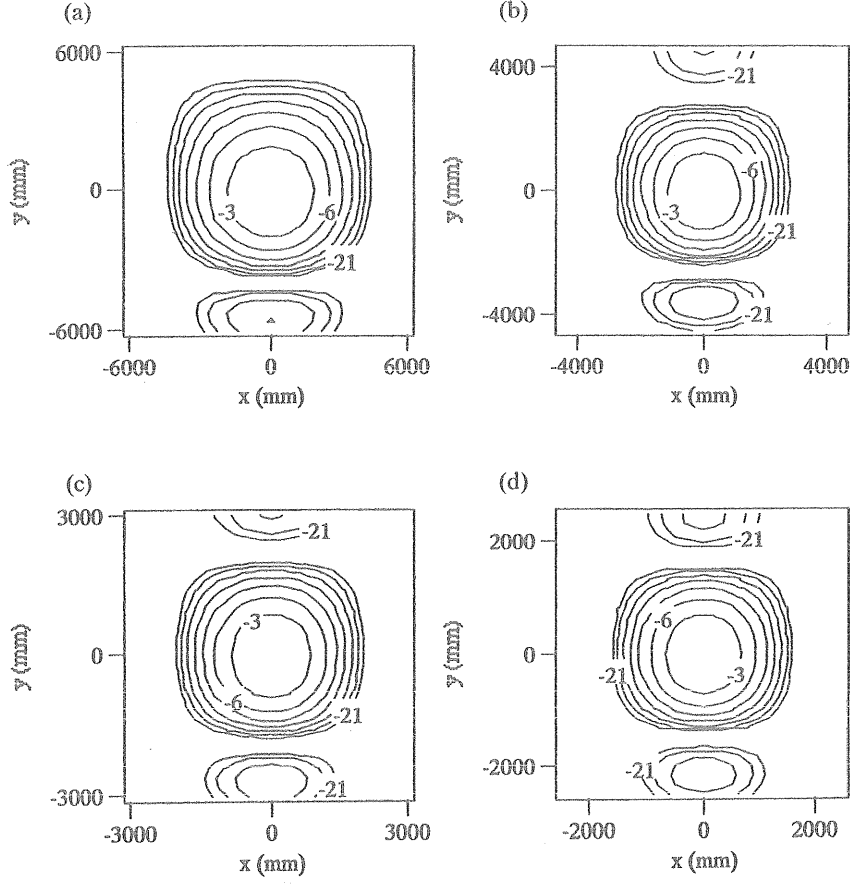


Figure 4. Calculated intensity contours in the far-field region. Distance from the image source is 100 m: (a) TE<sub>12</sub> mode (170 GHz); (b) TE<sub>13</sub> mode (271 GHz); (c) TE<sub>14</sub> mode (372 GHz); (d) TE<sub>15</sub> mode (472 GHz). Contours are in decibels relative to the intensity maximum.

Mode	Frequency (GHz)	$w_x$ (m)	$w_y$ (m)	$w_{x0}$ (mm)	$w_{y0}$ (mm)
TE <sub>02</sub>	223	1.61	2.38	26.6	18.0
TE <sub>03</sub>	323	1.13	1.64	26.2	18.0
TE <sub>04</sub>	423	0.85	1.25	26.5	18.0
TE <sub>12</sub>	170	3.09	3.14	18.2	17.9
TE <sub>13</sub>	271	1.92	1.94	18.3	18.1
TE <sub>14</sub>	372	1.40	1.42	18.3	18.0
TE <sub>15</sub>	472	1.12	1.12	18.1	18.0

Table 1. Spot sizes  $w_x$  and  $w_y$  in the far-field region ( $z = 100$  m) of the beam produced by image sources at various gyrotron operating modes and waist sizes  $w_{x0}$  and  $w_{y0}$  of equivalent bigaussian beam having its waist at the image source.

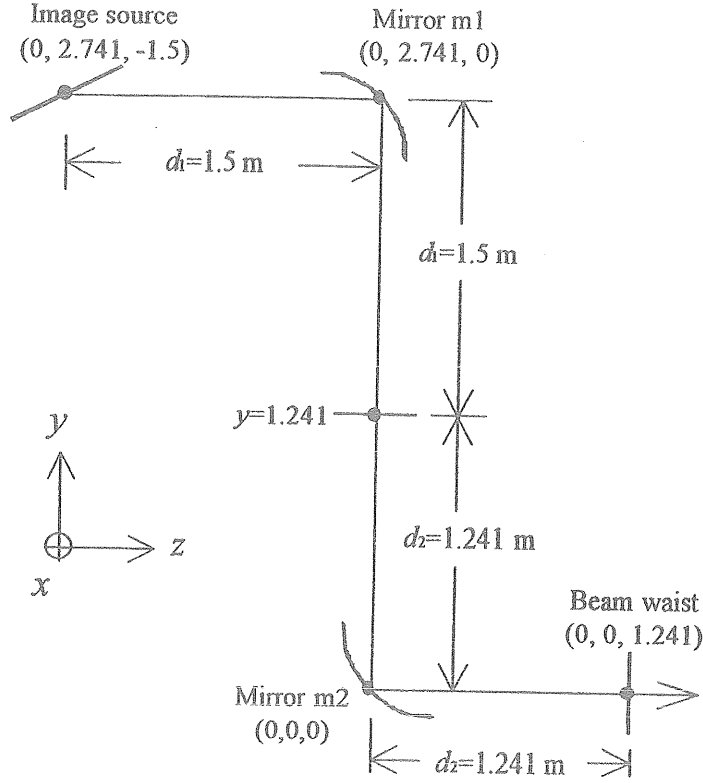


Figure 5. Quasi-optical system.

Treating the main beam as a bigaussian one with a waist at the position of the image source, the beam waist sizes  $w_{x0'}$  and  $w_{z0'}$  at the  $y = 1.241$  plane can be obtained from the relations

$$w_{x0'} = \frac{f_1 \lambda}{\pi w_{x0}} \quad w_{z0'} = \frac{f_1 \lambda}{\pi w_{y0}} \quad (5)$$

The equations show that since one waist is at the image source, the beam will have a waist at the  $y = 1.241$  plane. Because the mirror m2 has also the special arrangement ( $f_2 = d_2 = 1.241$  m), the beam will come to a waist at the  $z = 1.241$  plane. The final waist sizes  $w_{x0''}$  and  $w_{y0''}$  at the  $z = 1.241$  plane are given by

$$w_{x0''} = \frac{f_2}{f_1} w_{x0} \quad w_{y0''} = \frac{f_2}{f_1} w_{y0} \quad (6)$$

This result generally holds for a confocal system consisting of two mirrors. Note that it does not depend on frequency.

The focal lengths  $f_1$  and  $f_2$  are determined to be 1.5 m and 1.241 m, so this system produces a gaussian beam with the waist size  $w_{x0''} = w_{y0''} = 15.0$  mm for  $TE_{1n}$  mode. It also converts  $TE_{0n}$  mode gyrotron output into a bigaussian beam with the waist sizes  $w_{x0''} = 21.8$  mm and  $w_{y0''} = 14.9$  mm for  $TE_{0n}$  mode.

#### 4. Calculation results using the Huygens equation

The mirrors m1 and m2 are wide enough (m1 is 160 mm in width and 590 mm in length, while the corresponding dimensions for m2 are 170 mm and 240 mm) to avoid any diffraction losses due to the beam truncation. The shape of the mirror m1 is defined by an ellipse with focal points at  $(0, 2.741, -10)$  and  $(0, 0.976, 0)$  resulting in a focal length of  $f_1 = 1.5$  m. Analogously, the shape of the mirror m2 is defined also by an ellipse with focal points at  $(0, 10, 0)$  and  $(0, 0, 1.417)$  which gives a focal length of  $f_2 = 1.241$  m.

The intensity profiles at the  $y = 1.241$  plane for  $TE_{0n}$  modes are shown in figure 6 and those for  $TE_{1n}$  modes are presented in figure 7. Remembering that the  $x$ - and  $z$ -directions in figures 6 and 7 correspond to the  $x$ - and negative  $y$ -directions in figures 3 and 4, one can see that the corresponding intensity profiles are similar. The spot sizes  $w_x$  and  $w_z$  of the main beam agree well with the waist sizes  $w_{x0}$  and  $w_{z0}$  given by equation (5) (table 2). This corroborates that the radiation pattern produced at the  $y = 1.241$  plane is the far-field of the image source. As can be seen from the field

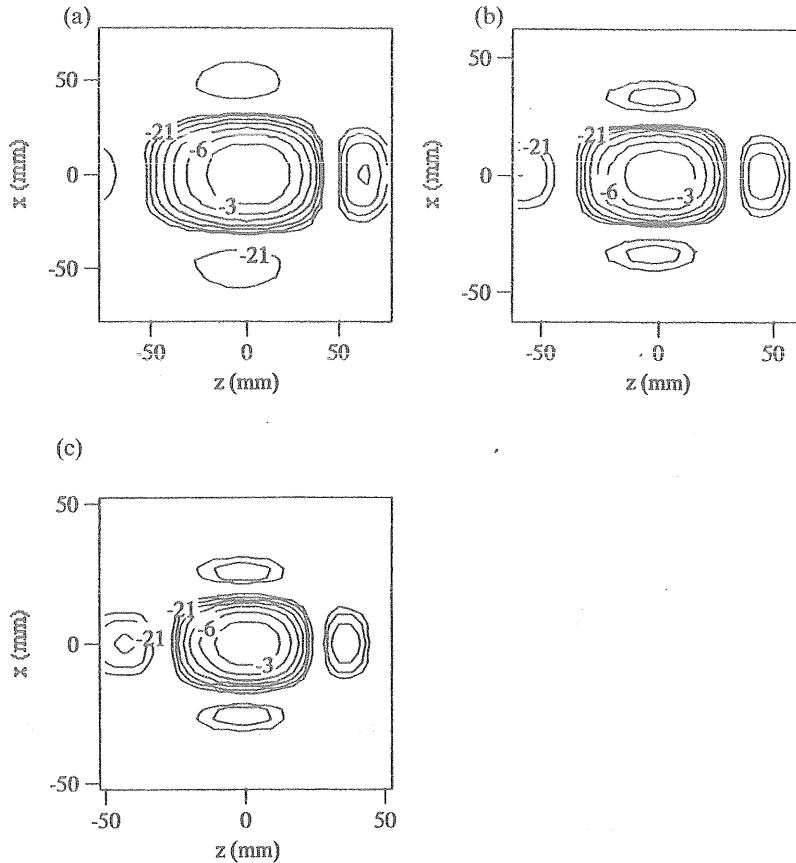


Figure 6. Calculated intensity contours at the  $y = 1.241$  plane: (a)  $TE_{02}$  mode (223 GHz); (b)  $TE_{03}$  mode (323 GHz); (c)  $TE_{04}$  mode (423 GHz). Contours are in decibels relative to the intensity maximum.



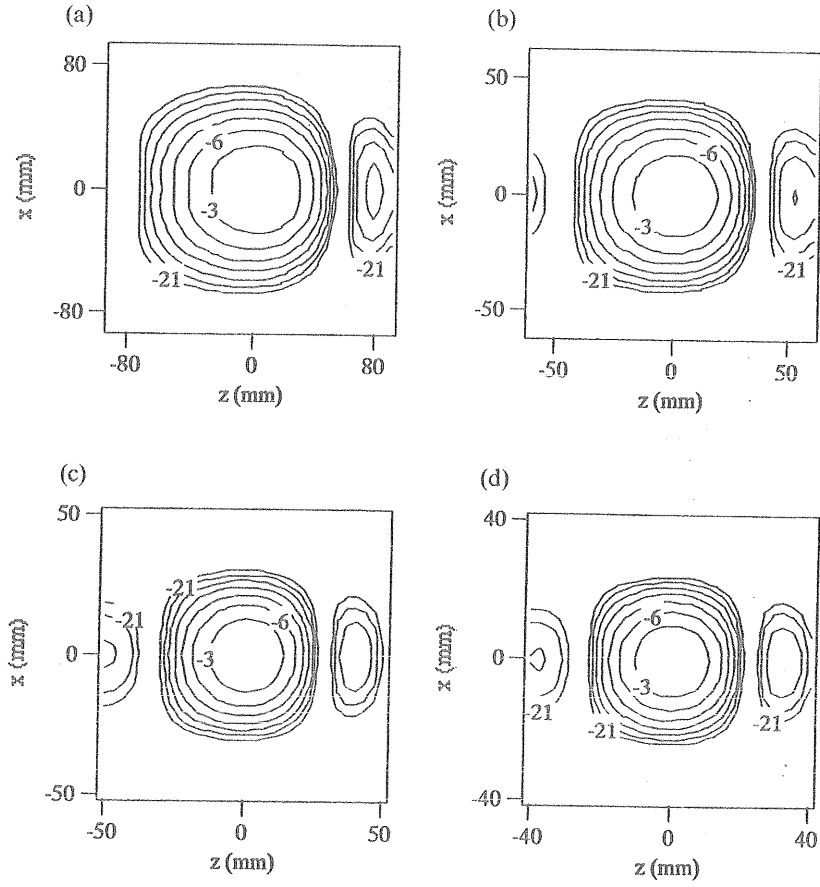


Figure 7. Calculated intensity contours at the  $y = 1.241$  plane: (a)  $TE_{12}$  mode (170 GHz); (b)  $TE_{13}$  mode (271 GHz); (c)  $TE_{14}$  mode (372 GHz); (d)  $TE_{15}$  mode (472 GHz). Contours are in decibels relative to the intensity maximum.

Mode	Gaussian optics				Calculation			
	$w_{x0'}$ (mm)	$w_{z0'}$ (mm)	$w_{x0''}$ (mm)	$w_{z0''}$ (mm)	$w_{x'}$ (mm)	$w_{z'}$ (mm)	$w_{x''}$ (mm)	$w_{z''}$ (mm)
$TE_{02}$	24.3	35.7	21.8	14.9	23.9	35.6	22.3	16.3
$TE_{03}$	16.8	24.6	21.8	14.9	17.0	25.0	24.1	16.5
$TE_{04}$	12.8	18.8	21.8	14.9	12.7	18.6	24.2	16.5
$TE_{12}$	46.6	46.6	15.0	15.0	46.8	45.0	16.2	16.2
$TE_{13}$	29.2	29.2	15.0	15.0	28.9	29.5	16.1	16.4
$TE_{14}$	21.3	21.3	15.0	15.0	21.0	21.4	16.4	16.4
$TE_{15}$	16.8	16.8	15.0	15.0	16.8	16.8	16.1	16.7

Table 2. Waist sizes obtained by gaussian optics and spot sizes obtained by numerical calculations of the Huygens equation. The values  $w_{x0'}$  and  $w_{z0'}$  are waist sizes at the filter and  $w_{x0''}$  and  $w_{z0''}$  are those at the waist, respectively. The values  $w_{x'}$  and  $w_{z'}$  are spot sizes at the filter and  $w_{x''}$  and  $w_{z''}$  are at the waist.

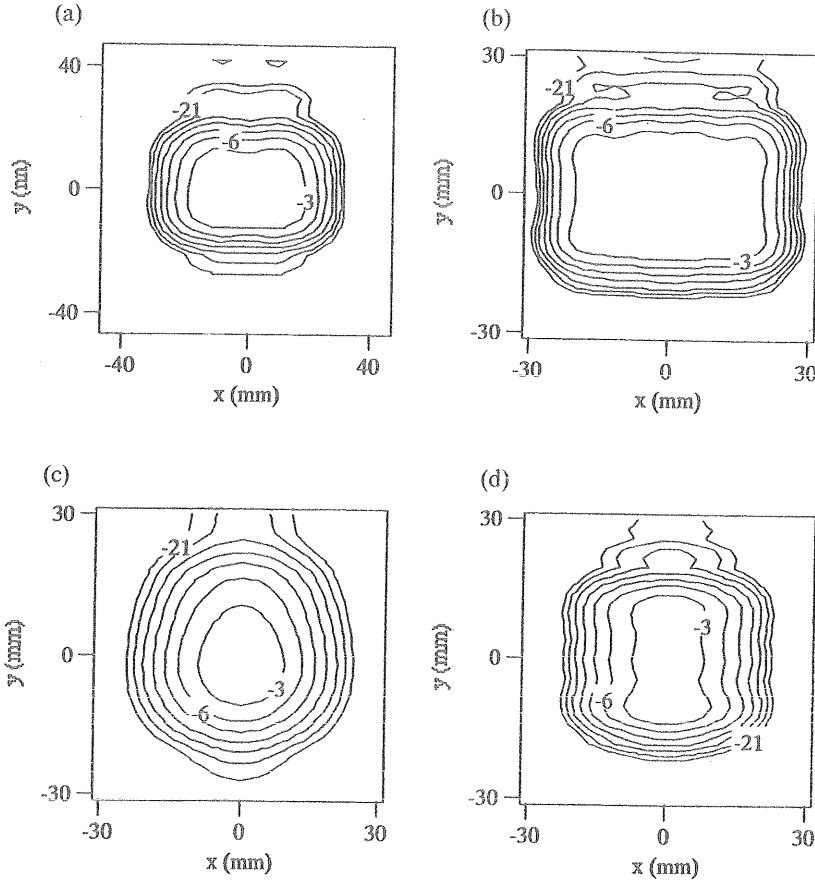


Figure 8. Calculated intensity contours at the beam waist without spatial filter: (a)  $TE_{02}$  mode (223 GHz); (b)  $TE_{04}$  mode (423 GHz); (c)  $TE_{12}$  mode (170 GHz); (d)  $TE_{15}$  mode (472 GHz). Contours are in decibels relative to the intensity maximum.

patterns (see for example figure 7) the sidelobes are not symmetrical due to the oblique position of the effective image source with respect to the  $z$ -axis.

The intensity profiles at the  $z = 1.241$  plane are shown in figure 8. Because their shapes are distorted by sidelobes seen in figures 6 and 7, they are quite different from a gaussian beam or a bigaussian beam. In order to improve the quality of the beams produced, it is necessary to remove the sidelobes from the far-field of the image source. Experimentally this can be done by inserting a spatial filter to block the sidelobes in the  $y = 1.241$  plane.

In principle, several loss-less methods can be used to transform any field distribution to gaussian beams (Bogdashov *et al.* 1995). Unfortunately these techniques are not broad band. Alternatively, it is justifiable to sacrifice a small amount of the beam power in order to improve beam quality through truncation of the sidelobes by a spatial filter. The main advantage of the latter approach is that by its nature it ensures broad-band operation of the system. Additionally, this conceptually simple solution can be realized very easily in practice.

Mode	$(x_c, y_c, z_c)$	$w_x$ (mm)	$w_z$ (mm)
TE <sub>02</sub>	$(0, 1.241, -5 \times 10^{-3})$	70	102
TE <sub>03</sub>	$(0, 1.241, -3 \times 10^{-3})$	50	70
TE <sub>04</sub>	$(0, 1.241, -2 \times 10^{-3})$	40	56
TE <sub>12</sub>	$(0, 1.241, -14 \times 10^{-3})$	140	140
TE <sub>13</sub>	$(0, 1.241, -6 \times 10^{-3})$	87	87
TE <sub>14</sub>	$(0, 1.241, -3 \times 10^{-3})$	62	62
TE <sub>15</sub>	$(0, 1.241, -4 \times 10^{-3})$	52	52

Table 3. The centre  $(x_c, y_c, z_c)$  of the plane and the sizes  $w_x, w_z$  in  $x$  and  $z$  directions for each mode.

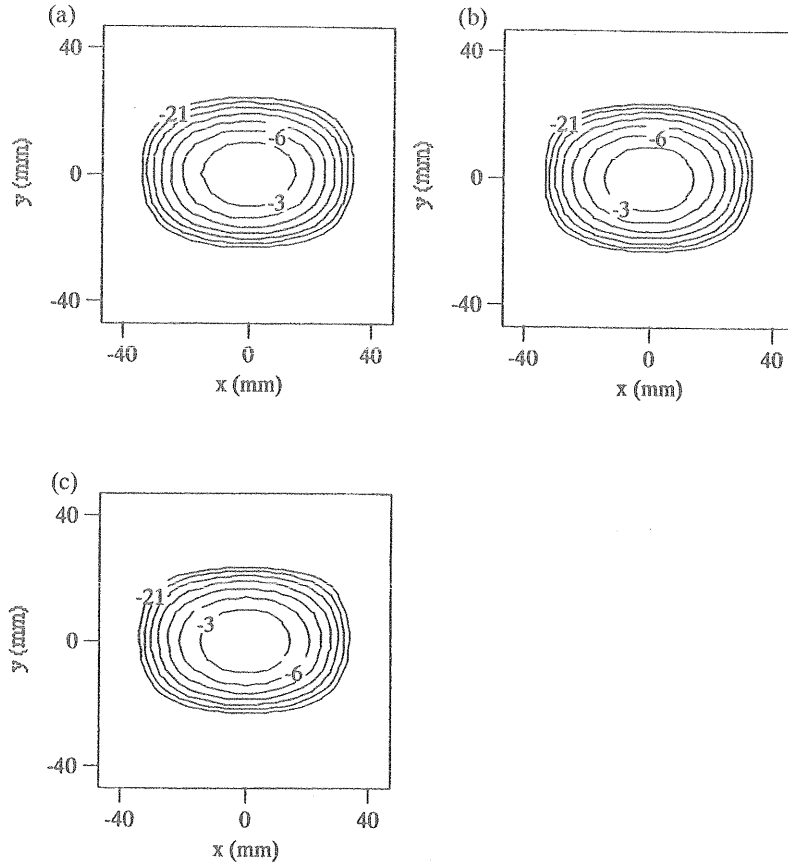


Figure 9. Calculated intensity contours at the output beam waist with spatial filter: (a) TE<sub>02</sub> mode (223 GHz); (b) TE<sub>03</sub> mode (323 GHz); (c) TE<sub>04</sub> mode (423 GHz). Contours are in decibels relative to the intensity maximum.

In our new conversion system the spatial filter used for removing the sidelobes is an indispensable component. It is just a thin plate with an aperture having dimensions  $w_x, w_z$  and centre in  $(x_c, y_c, z_c)$ . The filter is located at the  $y = 1.241$  plane. From the calculated field patterns in this cross-section an appropriate position and sizes of the aperture are selected in such a way as to block effectively only the sidelobes of the beam. More specifically, the aperture is selected large enough to encompass the  $-21$  dB contour of the main beam but small enough to truncate the  $-21$  dB contours of the sidelobes. The chosen parameters of the spatial filter are presented in table 3. Then the electromagnetic fields on the subsequent mirror m2 are calculated by using repeatedly the Huygens equation with fields at the aperture as sources.

The intensity profiles at the  $z = 1.241$  plane with spatial filtering for  $TE_{0n}$  modes are shown in figure 9 and those for  $TE_{ln}$  modes are shown in figures 10–13. One can

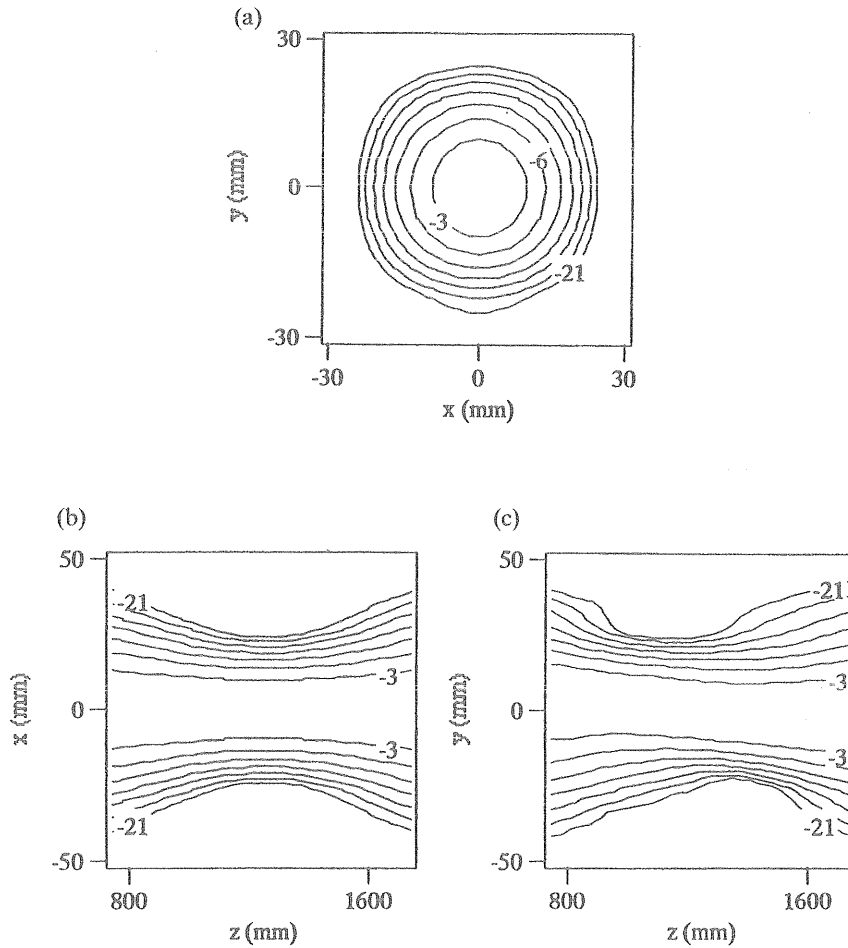


Figure 10. Calculated intensity contours for  $TE_{12}$  mode (170 GHz): (a) at the beam waist. Contours are in decibels relative to the intensity maximum; (b) and (c) in the vicinity of the beam waist. Contours are relative to the intensity along the  $z$ -axis.

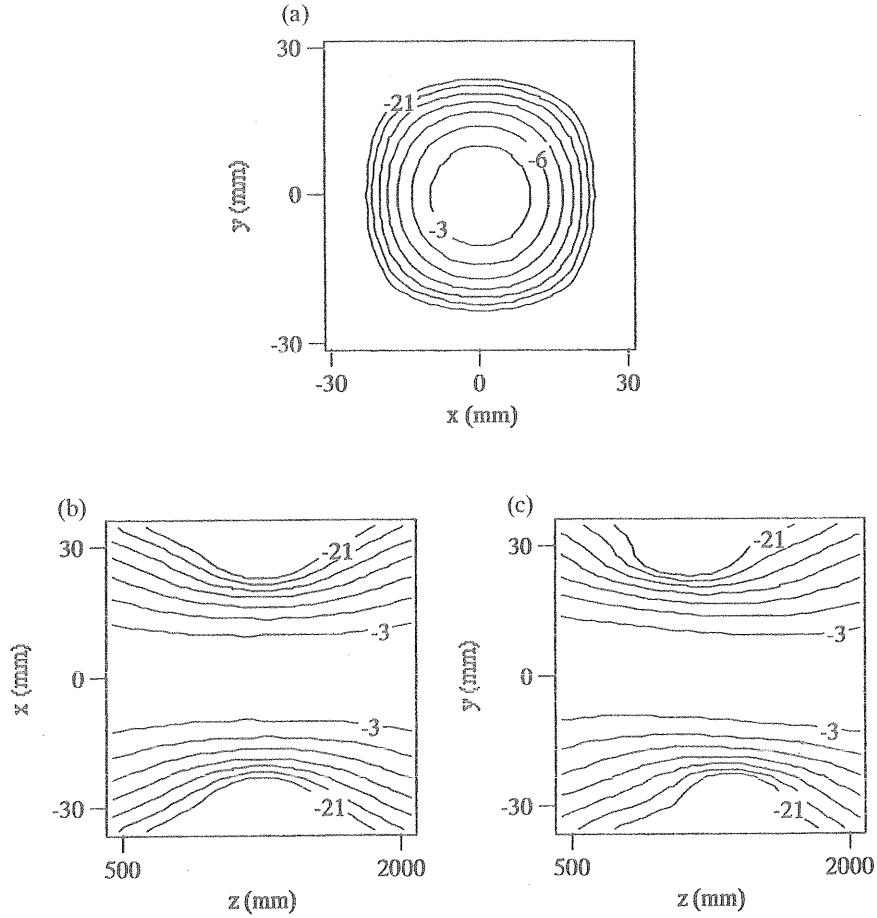


Figure 11. Calculated intensity contours for  $TE_{13}$  mode (271 GHz): (a) at the beam waist. Contours are in decibels relative to the intensity maximum; (b) and (c) in the vicinity of the beam waist. Contours are relative to the intensity along the  $z$ -axis.

see that this system converts four  $TE_{1n}$  mode outputs of the Gyrotron FU IVA into gaussian-like beams with waist size of  $w_{x''} = w_{y''} = 16.3$  mm as well as three  $TE_{0n}$  mode outputs into bigaussian-like beams with waist size of  $w_{x''} = 23.5$  mm and  $w_{y0''} = 16.4$  mm. The spot sizes  $w_{x''}$  and  $w_{y''}$  agree well with the waist sizes  $w_{x0''}$  and  $w_{y0''}$  given by equation (6) (table 2).

Most of the power (85% for  $TE_{0n}$  mode and 90% for  $TE_{1n}$  mode) from the image source still arrives at the beam waist in spite of the truncation of the sidelobes at the  $y = 1.241$  plane. It should be noticed that losses for different  $TE_{1n}$  modes differ insignificantly (less than 1%). The same applies to the  $TE_{0n}$  mode outputs.

## 5. Conclusion

The conversion system presented in this paper consists of a quasi-optical antenna, sequence of two ellipsoidal focusing mirrors and a spatial filter. It is

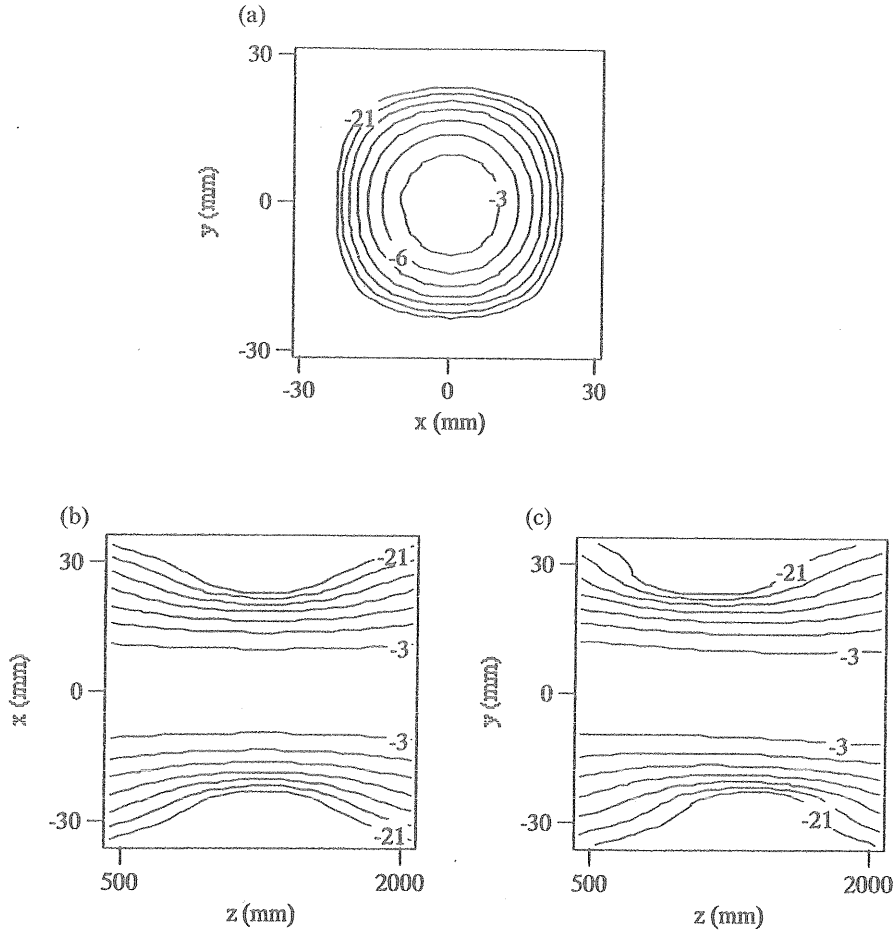


Figure 12. Calculated intensity contours for  $TE_{14}$  mode (372 GHz): (a) at the beam waist. Contours are in decibels relative to the intensity maximum; (b) and (c) in the vicinity of the beam waist. Contours are relative to the intensity along the  $z$ -axis.

intended to convert four  $TE_{1n}$  mode outputs of the Gyrotron FU IVA ( $TE_{12}$ , 170 GHz;  $TE_{13}$ , 271 GHz;  $TE_{14}$ , 372 GHz;  $TE_{15}$ , 472 GHz) into gaussian-like beams with waist size of  $w_{x''} = w_{y''} = 16.3$  mm as well as three  $TE_{0n}$  modes ( $TE_{02}$ , 223 GHz;  $TE_{03}$ , 323 GHz;  $TE_{04}$ , 423 GHz) into bigaussian-like beams with waist sizes of  $w_{x''} = 23.5$  mm and  $w_{y0''} = 16.4$  mm. Compared with the earlier system capable of converting only one operating mode the novel one is more versatile and is compatible with frequency tunable gyrotrons such as the Gyrotron FU IVA. In spite of the truncation of the sidelobes of the beam by the spatial filter most of the image source power is transferred to the final waist. As a result, intense high-quality beams in the submillimetre wavelength range can be produced.

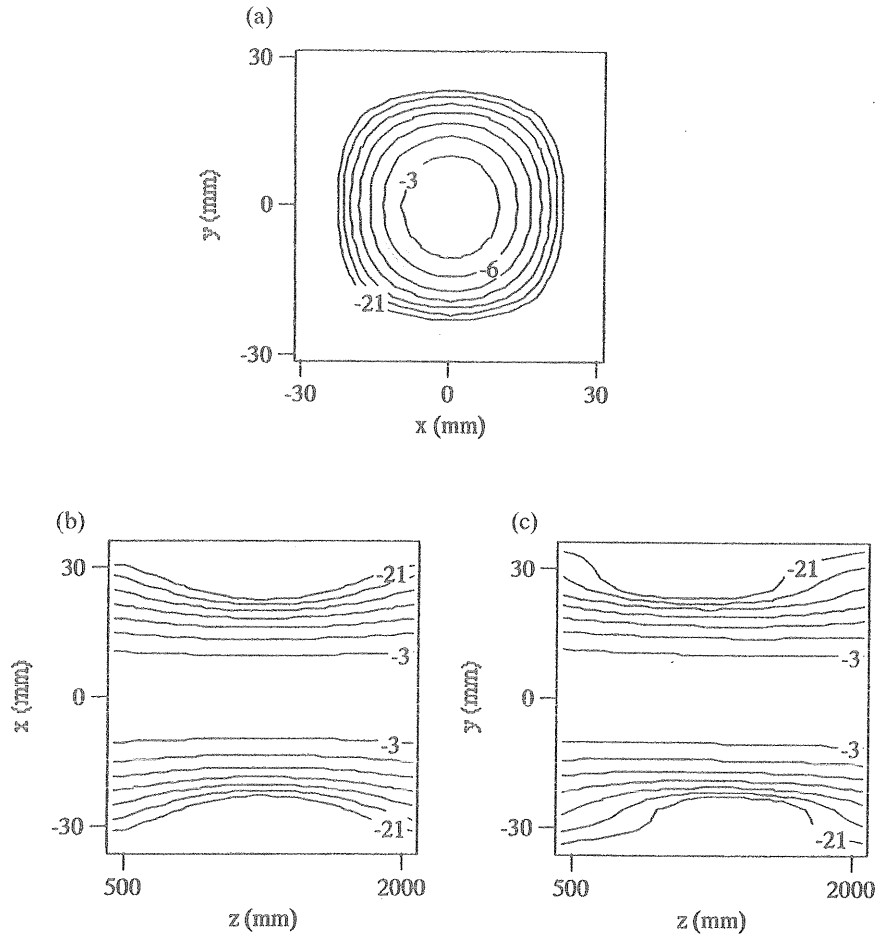


Figure 13. Calculated intensity contours for  $TE_{15}$  mode (472 GHz): (a) at the beam waist. Contours are in decibels relative to the intensity maximum; (b) and (c) in the vicinity of the beam waist. Contours are relative to the intensity along the z-axis.

#### Acknowledgments

This work was done as a collaboration between the Fukui University and the University of Stuttgart, Germany and was partially supported by a Grant-in-Aid from the Ministry of Education, Science and Culture of Japan and the Murata Science Foundation.

Numerical calculations were made at the Computer Center of the National Institute for Fusion Science.

#### References

- BOGDASHOV, A. A., CHIRKOV, A. V., DENISOV, G. G., VINOGRADOV, D. V., KUFTIN, A. N., MALYGIN, V. I., and ZAPEVALOV, V. E., 1995, Mirrors synthesis for gyrotron quasi-optical mode converters. *International Journal of Infrared and Millimeter Waves*, **16**, 735-744.

- BRAND, G. F., FEKETE, P. W., HONG, K., MOORE, K. J., and IDEHARA, T., 1990 b, Operating of a tunable gyrotron at the second harmonic of the electron cyclotron frequency. *International Journal of Electronics*, **68**, 1099–1111.
- BRAND, G. F., FEKETE, P. W., IDEHARA, T., and MOORE, K. J., 1990 a, Quasi-optical antennas for plasma scattering. *International Journal of Electronics*, **68**, 1063–1073.
- FEKETE, P. W., BRAND, G. F., and IDEHARA, T., 1994, Scattering from discrete Alfvén waves in a tokamak using a gyrotron radiation source. *Plasma Physics and Controlled Fusion*, **36**, 1407–1417.
- FLYAGIN, V. A., LUCHININ, A. G., and NUSINOVICH, G. S., 1983, Submillimeter-wave gyrotrons: theory and experiment. *International Journal of Infrared and Millimeter Waves*, **4**, 629–637.
- IDEHARA, T., NISHIDA, N., YOSHIDA, K., OGAWA, I., TATSUKAWA, T., WAGNER, D., GANTENBEN, G., KASPAREK, W., and THUMM, M., 1998, High frequency and high mode purity operations of Gyrotron FU IVA. *International Journal of Infrared and Millimeter Waves*, **19**, 919–930.
- IDEHARA, T., OGAWA, I., MITSUDO, S., PEREYASLAVETS, M., NISHIDA, N., and YOSHIDA, K., 1999, Development of frequency tunable, medium power gyrotrons (Gyrotron GU Series) as submillimeter wave radiation sources. *IEEE Transactions on Plasma Science*, **27**, 340–354.
- IDEHARA, T., SHIMIZU, Y., ICHIKAWA, K., MAKINO, S., SHIBUTANI, K., KURAHASHI, K., TATSUKAWA, T., OGAWA, I., OKAZAKI, Y., and OKAMOTO, T., 1995, Development of a medium power, submillimeter wave gyrotron using a 17 T superconducting magnet. *Physics of Plasmas*, **2**, 3246–3248.
- KONG, J. A., 1986, *Electromagnetic Wave Theory* (New York: Wiley and Sons).
- KREISCHER, K. E., and TEMKIN, R. J., 1987, Single-mode operation of a high-power, step-tunable gyrotron. *Physical Review Letters*, **59**, 547–550.
- NUSINOVICH, G. S., and READ, M. E., 1999, Theory of step-tunable gyrotrons operating at two cyclotron harmonics. *IEEE Transactions on Plasma Science*, **27**, 335–362.
- OGAWA, I., IDEHARA, T., MAEKAWA, S., KASPAREK, W., and BRAND, G. F., 1999 b, Conversion of gyrotron output into a gaussian beam using the far-field. *International Journal of Infrared and Millimeter Waves*, **20**, 801–821.
- OGAWA, I., IDEHARA, T., PEREYASLAVETS, M., and KASPAREK, W., 1999 a, Design of a quasi-optical system converting the TE<sub>06</sub> output mode of a gyrotron into a gaussian-like beam. *International Journal of Infrared and Millimeter Waves*, **20**, 543–558.
- OGAWA, I., SAKAI, A., IDEHARA, T., and KASPAREK, W., 1999 c, Application of the complex beam parameter to the design of quasi-optical transmission line for a submillimeter wave gyrotron. *International Journal of Electronics*, **86**, 1071–1084.
- OGAWA, I., SAKAI, A., IDEHARA, T., KAWAHATA, K., and KASPAREK, W., 1997, A quasi-optical transmission line for plasma scattering measurements using a submillimeter wave gyrotron. *International Journal of Electronics*, **83**, 635–644.
- SIEGMAN, A. E., 1971, *An Introduction to Lasers and Masers* (New York: McGraw-Hill).
- SPIRA-HAKKARAINEN, S., KREISCHER, K. E., and TEMKIN, R. J., 1990, Submillimeter-wave harmonic gyrotron experiment. *IEEE Transactions on Plasma Science*, **18**, 334–342.
- SUVOROV, E. V., HOLZHAUER, E., KASPAREK, W., LUBYAKO, L. V., BUROV, A. B., DRYAGIN, Y. A., FIL'CHENKOV, S. E., FRAIMAN, A. A., KUKIN, L. M., KOSTROV, A. V., RYNDYK, D. A., SHTANYUK, A. M., SKALYGA, N. K., SMOLYAKOVA, O. B., ERCKMANN, V., GEIST, T., KICK, M., LAQUA, H., and RUST, M., 1997, Collective Thomson scattering at WA-AS. *Plasma Physics and Controlled Fusion*, **39**, B337–B351.
- TERUMICHI, Y., KUBO, S., ANDO, A., YANAGIMOTO, Y., OGURA, K., TANAKA, H., TAKAHASHI, J., TONAI, I., NAKAMURA, M., MAEKAWA, T., TANAKA, S., and IDEHARA, T., 1984, Study of low frequency density fluctuations in the WT-2 tokamak by mm and submm wave scattering. *9th International Conference on Infrared and Millimeter Waves*, Takarazuka, Japan (Tokyo: Japan Society of Applied Physics), pp. 411–412.
- VLASOV, S. N., and ORLOVA, I. M., 1974, Quasioptical transformer which transforms the waves in a waveguide having a circular cross section into a highly directional wave beam. *Radiofizika*, **17**, 115–119.



- WADA, O., and NAKAJIMA, M., 1986, Reflector antennas for electron cyclotron resonance heating of fusion plasma. *Space Power*, **6**, 213-220.
- WOSKOBOINIKOW, P., COHN, D. R., and TEMKIN, R. J., 1983, Application of advanced millimeter/far-infrared sources to collective Thomson scattering plasma diagnostics. *International Journal of Infrared and Millimeter Waves*, **4**, 205-229.
- ZAYTSEV, N. I., PANKRATOVA, T. B., PETELIN, M. I., and FLYAGIN, V. A., 1974, Millimeter- and submillimeter-wave gyrotrons. *Radio Engineering and Electronic Physics*, **19**, 103-107.